

Structural, electronic, and magnetic properties of Sc_n ($n=2-18$) clusters from density functional calculations

Jinlan Wang

Department of Physics, Southeast University, Nanjing, 211189, People's Republic of China

(Received 2 October 2006; revised manuscript received 9 January 2007; published 19 April 2007)

The structural, electronic, magnetic properties of scandium clusters up to 18 atoms, within the framework of a gradient-corrected density functional theory, are reported. A number of low-lying isomers having different spin multiplicities are identified for each size. The clusters exhibit high stability at $n=4, 7, 10, 13,$ and $16,$ a result which can be interpreted in terms of atomic motif and electronic ordering (within the elliptical spherical jellium model). The computed average magnetic moment per atom of the lowest energy structure oscillates with cluster size and is as high as $1.5\mu_B$ for Sc_{13} . The measured magnetic moments are generally in accord with the average over different low-lying spin states of a given size. Ferromagnetic ordering is energetically preferred for smaller clusters with $n=2-8$ and competes with ferrimagnetic ordering in the medium sizes of $n=9-14$. Ferrimagnetic ordering is favored for larger sizes of $n=15-17$ and the first appearance of nonmagnetic state takes places at $n=18$, showing that the nonmagnetic character of bulk Sc is reached at relatively small cluster sizes.

DOI: [10.1103/PhysRevB.75.155422](https://doi.org/10.1103/PhysRevB.75.155422)

PACS number(s): 73.22.-f, 36.40.Cg, 75.75.+a

I. INTRODUCTION

The structure and magnetic properties of transition metal (TM) clusters have received considerable attention and a variety of interesting magnetic behavior different from the corresponding bulk solids have been identified.¹⁻⁸ For example, enhanced magnetic moments have been observed in small clusters of iron and cobalt,²⁻⁴ and ferromagnetic or ferrimagnetic ordering has been identified in chromium (Cr_8 - Cr_{156}) and manganese (Mn_5 - Mn_{99}) clusters, even though Cr and Mn are both antiferromagnetic in the bulk phase.^{2,5} Substantial nonzero moments have also been found for Rh_{9-60} clusters even though bulk rhodium is paramagnetic at all temperatures.⁶ As with most transition elements, scandium is paramagnetic in the bulk phase while recent Stern-Gerlach molecular-beam deflections studies have indicated that small scandium clusters are magnetic ordering in the range of $n=5-20$ and the magnetic moment is as high as $6.0\pm 0.2\mu_B$ for the Sc_{13} cluster.⁷

Transition metal clusters are challenging systems for theoretical studies because their partly filled d shells typically result in a number of alternative low-lying isomers within a very narrow energy range. Although the electronic configuration of an isolated scandium atom is simple ($3d^14s^2$), only a few computations have been made on the smallest scandium dimer and trimer thus far.⁹⁻¹⁹ Meanwhile, there has been no theoretical investigation of magnetism of scandium clusters of any size to date. Therefore, it is desirable to extend the study of scandium clusters to larger sizes so as to glean a comprehensive understanding of their structures and properties. In this paper, we systematically explore the structural, energetic, electronic, and magnetic properties of Sc_n , $n=2-18$ using a gradient-corrected density functional theory (DFT). The size-dependent binding energy, highest-occupied-molecular-orbital-(HOMO-) lowest-unoccupied-molecular-orbital (LUMO) gap, spin stability, and magnetic moment are discussed.

II. COMPUTATIONAL METHOD

The reliability of DFT studies depends on the choice of the functional and the basis set for the problem being investigated. We employ the Perdew-Burke-Ernzerhof²⁰ (PBE) parametrization of the exchange-correlation functional as well as a DFT-based relativistic semi-core pseudopotential²¹ (DSPP), fitted to all-electron relativistic results, and a double numerical basis set including d -polarization functions (DND), as implemented in the DMOL package.²²

The accuracy of the PBE/DSPP/DND combination is evaluated by the computations on small Sc_n , $n=1-3$. For an isolated scandium atom, the current computational scheme predicts the ground electron spin state as a doublet state and the ionization potential of 6.729 eV, which agrees well with the measured results (2D_g , 6.565 eV).²³ For the scandium dimer, the quintet state is energetically preferred than the triplet state by 0.027 eV in this calculation which is in accord with earlier DFT results.¹³⁻¹⁵ The computed dissociation energy of 1.364 eV and vibrational frequency of 261.0 cm^{-1} are well reproduced in comparison with the measured values of 1.65 ± 0.22 eV and 239.9 cm^{-1} , respectively.^{24,25} The predicted bond length of 2.64 Å is also within the range of 2.56–2.65 Å reported earlier.¹⁶⁻¹⁸ As for scandium trimer, the lowest energy structure is an equilateral triangle in a doublet state with the bond length of 2.82 Å. The next low-lying isomer is an isosceles triangle with the bond length of 2.71 Å with an angle of 64.4°. This isosceles triangle is in a doublet state with 0.017 eV higher in energy than the most stable structures. An obtuse isosceles triangle with the bond length of 2.76 Å and the vertex angle of 69.0° in a quartet state is 0.228 eV higher than the ground state. This structure is distorted from the equilateral triangle because of the Jahn-Teller effect. Most of earlier DFT and high-level multireference computations^{9,10,14,19} have also predicted that the doublet equilateral triangle is the best structure and the bond lengths are in the range of 2.81–3.04 Å. However, the quartet C_{2v} structure has been reported to be more stable than the

doublet found in earlier BP86 computations.¹⁶

The number of distinct initial geometries is important to the reliability of the ground state structures obtained. For the clusters with the size smaller than eight atoms, we construct the possible conformations by hand. For the clusters with the size larger than eight atoms, the initial geometries are prepared from titanium cluster generated from a genetic algorithm based on an empirical tight-binding potential.^{26–29} Eight arbitrary configurations are used as the initial population. Two configurations from this population are chosen randomly as parents to produce an offspring through the mating and mutation procedure. The offspring cluster is then relaxed using molecular dynamics techniques. If the energy of the offspring is lower than that of at least one of the parents, the offspring take the place of the parent with the higher energy. Four to six distinct low-energy configurations are generated in this way for each size. Considering the bond length of Sc-Sc is about 1.1 times longer than that of Ti-Ti, we rescale the Cartesian coordinates of all the atoms by a factor of 1.1. All the structures are then fully optimized at PBE/DSPP/DND level by considering different spin multiplicities without symmetry restriction. The stability of the lowest energy structures/states obtained are further confirmed to be the minima of the potential energy surface of Sc clusters by harmonic frequency computations.

III. RESULTS AND DISCUSSION

A. Isomers and corresponding spin states of Sc_n ($n=2-18$)

The structures, binding energies, and HOMO-LUMO gaps of the low-lying isomers of Sc_n , $n=2-18$, are presented in Table I. The lowest energy structure and the corresponding symmetry of each size are displayed in Fig. 1. Results for the scandium dimer and trimer are discussed in the computational method section and are not repeated here. For the tetramer, the most stable structure is a tetrahedron with D_{2d} symmetry in a triplet state, with a singlet tetrahedron having C_{2v} symmetry lying 0.132 eV higher in energy. For Sc_5 , a triangular bipyramid (C_{2v}) in a doublet state is more stable than a similar structure in a quartet state by 0.09 eV. For the case of Sc_6 , a triplet octahedron with C_{2h} symmetry is found to be energetically favored over a singlet octahedron having D_{2h} symmetry by 0.096 eV. Another quite distorted octahedron in a triplet state is also found to be a minimum and it is 0.188 eV above the ground state structure. For Sc_7 , a doublet pentagonal bipyramid with D_{5h} symmetry is more stable than a quartet having similar structure by 0.07 eV. The bond lengths of these two isomers are very close differing by, less than 0.008 Å.

Three energetically degenerate isomers having different spin multiplicities are obtained for Sc_8 . The geometries of these three isomers are all in C_{2v} symmetry and can be viewed as bicapped octahedrons. The quintet state is found to be more stable than the triplet and singlet state by 0.016 and 0.024 eV (only 0.002 and 0.003 eV per atom) in energy, respectively. For Sc_9 , the lowest energy structure is a singly capped tetragonal prism structure in a doublet state. A similar singly capped tetragonal prism but in a quartet state is energetically quasidegenerate with the doublet state, with the en-

ergy difference of 0.027 eV. A bicapped pentagonal bipyramid in a doublet state lies higher in energy ($\Delta E=0.18$ eV) with respect to the lowest energy structure. Another similar bicapped pentagonal bipyramid in a quartet state is much higher energy ($\Delta E=0.27$ eV). Two tri-capped octahedrons in a doublet and a quartet state are also found to be low-lying isomers with 0.252 and 0.279 eV higher in energy above the ground state structure, respectively.

The lowest energy structure of Sc_{10} can be described as interpenetrating-pentagonal bipyramid in a triplet state. A similar conformation but in a singlet state is only 0.01 eV higher in energy. A tricapped pentagonal bipyramid structure in a triplet state is energetically unfavorable as compared to the ground state structure ($\Delta E=0.25$ eV). For Sc_{11} , a triple tetracapped pentagonal bipyramid structure is the most favorable structure and is followed by a similar packing in a doublet state lying very close in energy ($\Delta E=0.044$ eV). A capped distorted anti-five-prism in a quartet state is found to be less stable than the ground state by 0.121 eV. A similar geometry but in a doublet state is 0.154 eV higher in energy above the ground state. The energetically preferred structure for Sc_{12} is a distorted bell-like conformation in a quintet state. The triplet state and the singlet counterparts are only 0.049 and 0.082 eV higher in energy, respectively. For the case of Sc_{13} , the lowest energy structure is very close to I_h structure (within 0.05 Å tolerance) with a remarkably high total magnetic moment $19\mu_B$. The nearest distances between surface Sc atoms and surface-core atoms in this lowest energy icosahedron are 3.156 and 3.002 Å, respectively. The second lowest energy structure also possesses relative high magnetic moment as high as $17\mu_B$ and the energy difference is 0.142 eV. The states of 15 and $13\mu_B$ lie above the ground state by 0.339 and 0.446 eV, respectively. The other low spin states ($\mu=11-1\mu_B$) (see Table I) are found much less stable with the energy difference larger than 0.55 eV. A cubic structure in a quartet state is also found to possess much higher energy ($\Delta E=1.186$ eV) as shown in Table I. A face-capped icosahedron is obtained as the lowest energy structure for Sc_{14} and the best spin state is a nonet state. The triplet is less stable by 0.032 eV while the quintet and septet state are disfavored by 0.085 and 0.086 eV higher in energy, respectively. In the case of Sc_{15} , a quartet body-centred cubicle structure with C_{2v} symmetry is the most stable structure whereas the doublet counterpart is only 0.09 eV above in energy. In the case of Sc_{16} , the energetically preferred structure is a tricapped icosahedron in a singlet state. The triplet state and the quintet state are unfavorable by 0.048 and 0.096 eV higher in energy. A near-spherical compact structure in a doublet state is found as the most stable structure for Sc_{17} . This structure can be built on the basis of a distorted icosahedron by adding four capping atoms. A low-lying isomer in a quartet state is also identified and its energy is 0.093 eV higher above the ground state. The biggest cluster studied in this work is Sc_{18} . The lowest energy structure of Sc_{18} is a bell-like conformation in a singlet state. The triplet state lies with 0.05 eV higher in energy. These two bell-like conformations are in fact the same and can be viewed as truncated-apex icosahedrons. A quintet icosahedronlike structure is less stable than the ground singlet state by 0.152 eV higher in energy.

TABLE I. The structure/symmetry, the spin multiplicity, the average binding energy per atom, and the HOMO-LUMO gap of the lowest energy structure and metastable structures of Sc_n $n=2-18$ clusters.

System	Structure (symmetry)	Multiplicity	E_b (eV/atom)	Gap (eV)
Sc_2	D_∞	5	1.009	0.278
	D_∞	3	0.872	0.176
Sc_3	Equilateral triangle (D_{3h})	2	1.569	0.504
	Isosceles obtuse triangle (C_{2v})	2	1.563	0.550
	Isosceles obtuse triangle (C_{2v})	4	1.493	0.344
Sc_4	Tetrahedron (D_{2d})	3	2.042	0.446
	Tetrahedron (C_{2v})	1	2.009	0.281
Sc_5	Triangular bipyramid (C_{2v})	2	2.289	0.322
	Triangular bipyramid (C_{2v})	4	2.271	0.196
Sc_6	Octahedron (C_{2h})	3	2.458	0.222
	Octahedron (D_{2h})	1	2.442	0.242
	Octahedron (C_{2v})	3	2.427	0.235
Sc_7	Pentagonal bipyramid (D_{5h})	2	2.636	0.270
	Pentagonal bipyramid (D_{5h})	4	2.626	0.221
Sc_8	Two capped octahedrons (C_{2v})	5	2.715	0.274
	Two capped octahedrons (C_{2v})	3	2.713	0.332
	Two capped octahedrons (C_{2v})	1	2.712	0.265
Sc_9	Singly capped tetragonal prism (C_s)	2	2.769	0.258
	Singly capped tetragonal prism (C_s)	4	2.766	0.156
	Two capped pentagonal bipyramid (C_1)	2	2.749	0.369
	Two capped pentagonal bipyramid (C_1)	4	2.739	0.119
	Tricapped octahedron (C_1)	2	2.741	0.139
	Tricapped octahedron (C_1)	4	2.738	0.178
Sc_{10}	Interpenetrating pentagonal bipyramid (C_1)	3	2.841	0.217
	Interpenetrating pentagonal bipyramid (C_1)	1	2.840	0.210
	Tricapped pentagonal bipyramid (C_1)	3	2.816	0.229
Sc_{11}	Tetracapped pentagonal bipyramid (C_2)	2	2.885	0.250
	Tetracapped pentagonal bipyramid (C_2)	4	2.881	0.183
	Capped anti-five-prism (C_{2v})	4	2.874	0.103
	Capped anti-five-prism (C_{2v})	2	2.871	0.174
Sc_{12}	Bell-shaped structure (C_1)	5	2.972	0.185
	Bell-shaped structure (C_1)	3	2.968	0.247
	Bell-shaped structure (C_1)	1	2.964	0.154
Sc_{13}	Icosahedron (C_{2h})	20	3.105	0.296
	Icosahedron (C_1)	18	3.094	0.090
	Icosahedron (C_1)	16	3.079	0.152
	Icosahedron (C_1)	14	3.071	0.141
	Icosahedron (C_1)	10	3.062	0.220
	Icosahedron (C_1)	12	3.060	0.121
	Icosahedron (C_s)	8	3.055	0.213
	Icosahedron (D_{3d})	6	3.027	0.127
	Icosahedron (C_{2h})	2	3.021	0.150
	Icosahedron (C_{2h})	4	3.017	0.147
	Icosahedron (C_i)	22	3.020	-0.313 ^a
	Cubic (D_{2h})	4	3.030	0.205

TABLE I. (Continued.)

System	Structure (symmetry)	Multiplicity	E_b (eV/atom)	Gap (eV)
Sc ₁₄	Capped icosahedron (C_1)	9	3.086	0.145
	Capped icosahedron (C_1)	3	3.084	0.243
	Capped icosahedron (C_1)	1	3.081	0.239
	Capped icosahedron (C_1)	7	3.080	0.130
	Capped icosahedron (C_1)	5	3.080	0.153
Sc ₁₅	Body-centred cubic (C_{2v})	4	3.118	0.221
	Body-centred cubic (C_{2v})	2	3.112	0.154
Sc ₁₆	Tricapped icosahedron (C_1)	1	3.157	0.171
	Tricapped icosahedron (C_1)	3	3.154	0.158
	Tricapped icosahedron (C_1)	3	3.151	0.152
Sc ₁₇	Near-spherical tetracapped icosahedron (C_1)	2	3.218	0.159
	Near-spherical tetracapped icosahedron (C_1)	4	3.194	0.131
Sc ₁₈	Bell-like structure (C_1)	1	3.221	0.145
	Bell-like structure (C_1)	3	3.218	0.116
	Uncompleted double icosahedron (C_1)	5	3.212	0.087

^aThe HOMO-LUMO gap is negative indicating this spin state is not the correct one in terms of wave function stability.

B. Binding energy

The average binding energy per atom of the lowest energy structures determined for Sc_{*n*} clusters is plotted in Fig. 2(a) as a function of the cluster size. The average binding energy increases rapidly from 1.009 eV for the dimer to 2.042 eV for the tetramer which corresponds to the structural transition from two to three dimensions. The average binding energy of the cluster increases gradually in the range $n=4-12$. The curve of $E_b(n)$ exhibits a prominent peak at $n=13$, indicating that Sc₁₃ possesses unusually high stability. For the large sizes of $n=13-18$, the increase of $E_b(n)$ becomes more gradual; the average binding energy of Sc₁₈ is 3.221 eV which is approaching the bulk value (3.9 eV).³⁰

To further illustrate the stability of the cluster and the size-dependent behavior, we investigate the second difference in energy $\Delta_2 E(n)$ as a function of size. The $\Delta_2 E(n)$ is a quantity frequently used as a measure of the relative stability of the cluster and is often compared directly with the relative abundances determined in mass spectroscopy experiments. It is defined as

$$\Delta_2 E(n) = E(n+1) + E(n-1) - 2E(n), \quad (1)$$

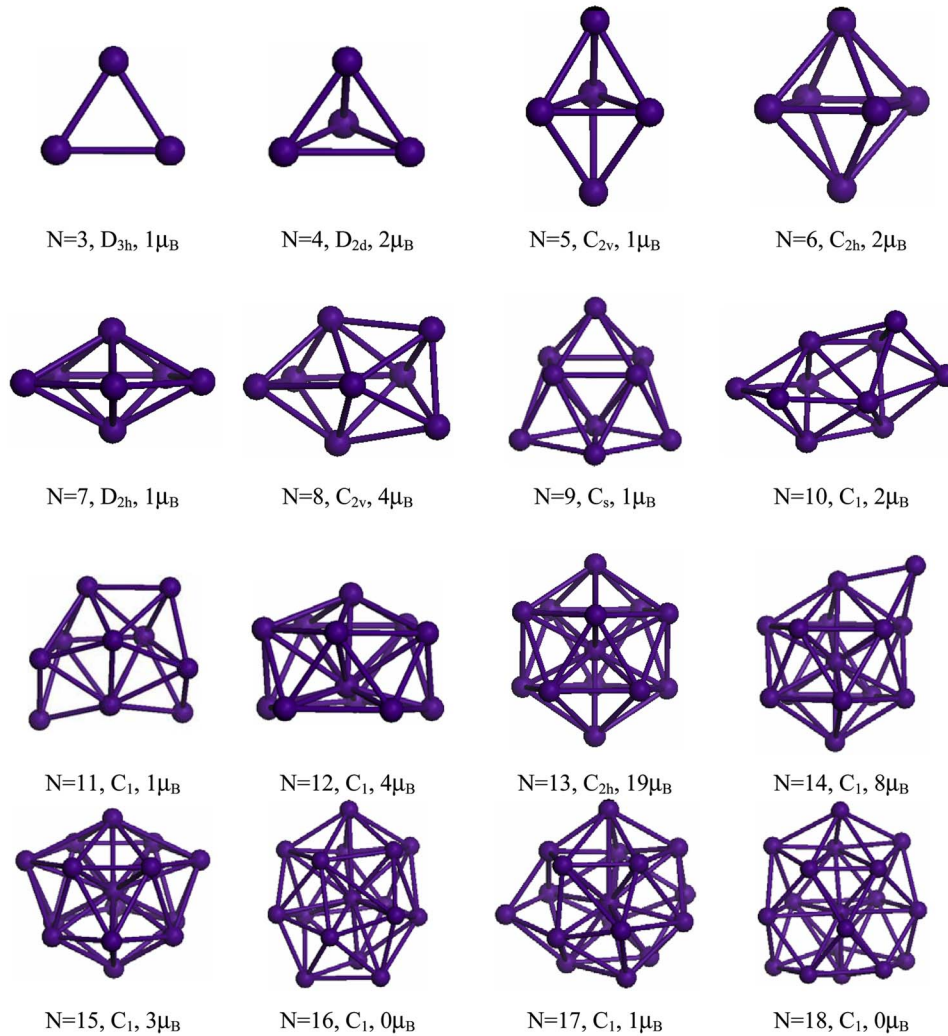
where $E(n)$ is the total energy of an n -atom cluster. As shown in Fig. 2(b), particularly prominent maxima for $\Delta_2 E(n)$ are found at $n=4, 7, 13$, indicating these clusters are more stable than their neighbors. The highly stability of these clusters might stem from their highly symmetric close-packed geometries which, for the lowest energy structures, are the tetrahedron, pentagonal bipyramid and icosahedron, respectively. By contrast, the geometries of Sc₁₂ and Sc₁₄ can be viewed as an icosahedron by truncating an apex or by adding an additional atom which likely reduces the stability of these two clusters and explaining why $\Delta_2 E(n)$ peaks at $n=13$.

Other local peaks in $\Delta_2 E(n)$ are found at $n=10$ and 16 which suggests that Sc₁₀ and Sc₁₆ are also more stable than their neighboring sizes $n=9, 11$ and $n=15, 17$. Considering that the valence electronic configuration of scandium atom is $3d^1 4s^2$, the total numbers of the valence electrons of Sc₁₀ and Sc₁₆ are 30 and 48, respectively, which are consistent with the closure of the electronic shells within the elliptical spherical jellium model. Therefore, there exist two effects, atomic motif and electronic ordering, in determining the stability of small scandium clusters with the atomic motif playing a dominant role.

C. HOMO-LUMO gap and spin stability

The HOMO-LUMO gap is a characteristic quantity of metal clusters' electronic structure and is a commonly used measure of the ability for clusters to undergo activated chemical reactions with small molecules. From Table I, it is seen that the HOMO-LUMO gaps are relatively small (around 0.1–0.3 eV) for all of the Sc_{*n*} clusters containing more than five atoms. This might be cited as one of the indicators of metallic behavior, appearing even in very small clusters. No simple correlation between the HOMO-LUMO gap and the spin-multiplicity state is observed for a given Sc_{*n*} cluster (see Table I). The HOMO-LUMO gaps of the lowest energy structures of Sc_{*n*}, $n=2-18$, are presented as a function of cluster size in Fig. 3. The gap shows a decreasing tendency over the sizes studied in this work although local maximums are found for $n=4$ and 13 indicative of the extra high stability of Sc₄ and Sc₁₃ in terms of atomic packing.

In theoretical studies of clusters, the spin gaps δ_1 , δ_2 are commonly defined as

FIG. 1. (Color online) The lowest energy structures of Sc_n ($n=2-18$).

$$\delta_1 = -[\epsilon_{\text{HOMO}}^{\text{majority}} - \epsilon_{\text{LUMO}}^{\text{minority}}], \quad \delta_2 = -[\epsilon_{\text{HOMO}}^{\text{minority}} - \epsilon_{\text{LUMO}}^{\text{majority}}] \quad (2)$$

are used to evaluate the spin stability of the cluster. Generally a given spin arrangement is classified as magnetic stable if δ_1 and δ_2 are both positive. Namely, magnetic stability occurs when the LUMO of the majority manifolds (spin up) lies above the HOMO of the minority (spin-down) manifolds and *vice versa*. We depict the spin gaps δ_1 and δ_2 of the ground state structures of the Sc_n clusters in Fig. 3. One can clearly see that both δ_1 and δ_2 are positive for $n=2-18$, indicating that all the Sc clusters studied in this article are magnetic stable. Interestingly, both δ_1 and δ_2 decrease rapidly in the range of $n=2-5$ and continues to decrease with increasing cluster size. However, δ_2 shows extra high local peaks at $n=8, 13$, and is correlated with the relatively high magnetic moments and the highly symmetric geometries are obtained for these clusters.

D. Size-specified magnetic moments

To investigate the size-dependent magnetic properties, we have computed the average magnetic moment per atom of

the lowest energy structure of Sc_n shown in Fig. 4. As shown in the figure, the average magnetic moment of the Sc clusters oscillates significantly with the size. In the size range $n \leq 12$, relatively large average magnetic moments are found for clusters with even number of atoms whereas the odd- n clusters possess smaller magnetic moments. For instance, the average magnetic moment of Sc_n , $n=2, 4, 6, 8, 10, 12, 14$ is 2.0, 0.5, 0.33, 0.5, 0.33, 0.57 μ_B , respectively, while it reduces to only 0.2 μ_B in Sc_7 and Sc_9 . A particularly high magnetic moment, 1.5 μ_B per atom, is obtained for Sc_{13} . The magnetic moments of the clusters becomes quite small for Sc_{16-18} , (around 0.06 μ_B /per atom for Sc_{17} and zero for $Sc_{16,18}$), an observation in accord with an evolution toward the paramagnetic behavior of the bulk.

In comparison with the measured data,⁷ our prediction of the magnetism is reproduced well at $n=5, 7, 9, 11, 17$, with discrepancies of less than 0.03 μ_B /per atom for these five cases. However, the deviation between the computational and experimental results are more substantial for $n=6, 8, 15, 16, 18$ and are particularly large for $n=13, 14$. For Sc_{13} and Sc_{14} , the computed average magnetic moments are predicted to be 1.5 and 0.57 μ_B per atom whereas the Stern-

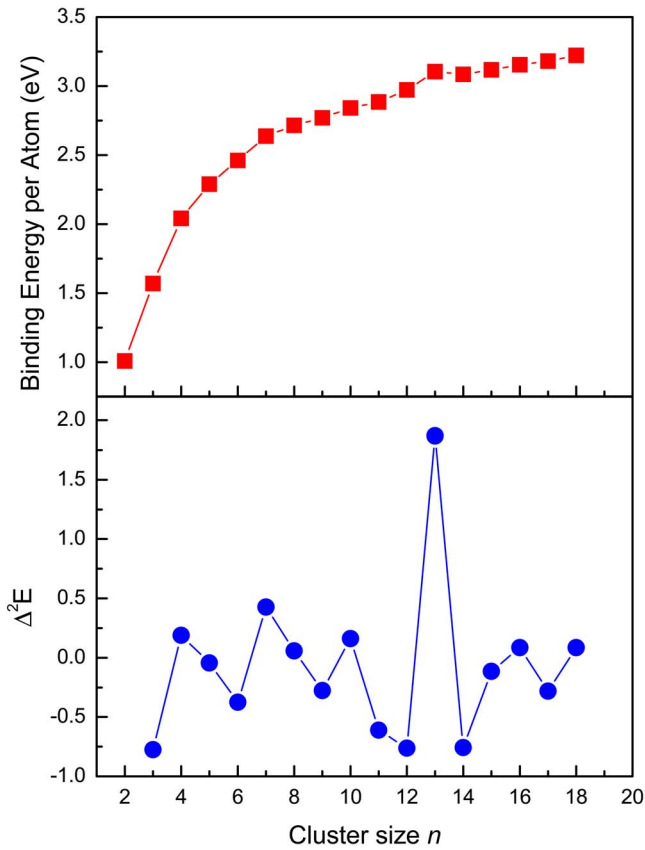


FIG. 2. (Color online) The average binding energy per atom and the second energy difference of the lowest energy structure of Sc_n are plotted as functions of cluster size.

Gerlach experiments⁷ indicate values of only 0.56 and $0.13\mu_B$, respectively. We now consider possible explanations for the discrepancies between the theoretically calculated moments and the experimental measurements.

As discussed above, a number of nearly degenerate structures of a given n , but having different spin states were iden-

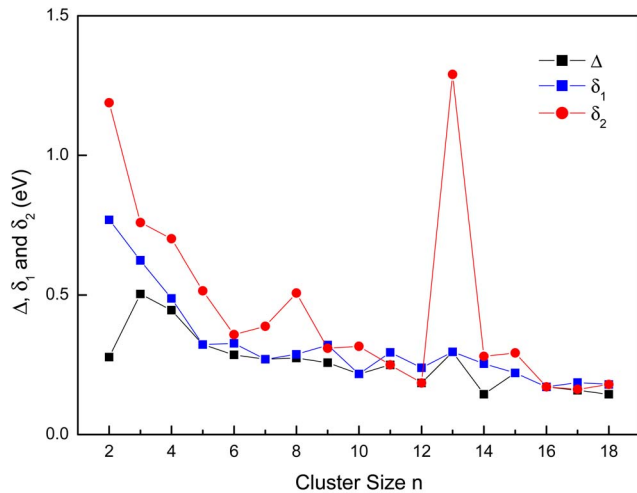


FIG. 3. (Color online) The HOMO-LUMO gap and spin gaps of the lowest energy structure of Sc_n plotted as a function of cluster size n .

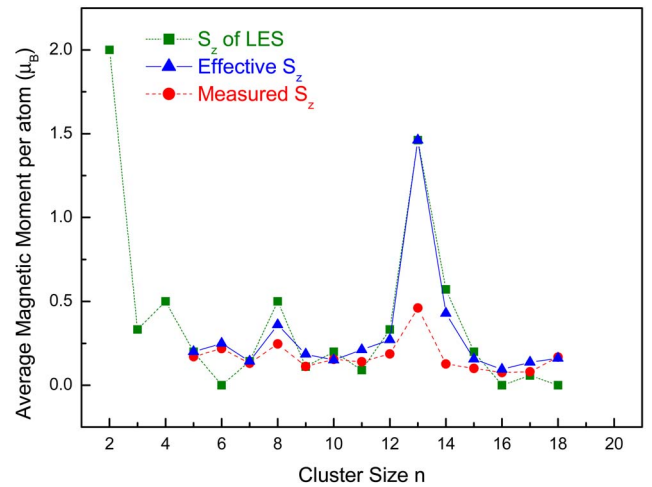


FIG. 4. (Color online) The computed per-atom magnetic moments of the lowest energy structure (LES), and the effective average magnetic moment computed as a multiplicity-weighted average over different low-energy structures presented as functions of the cluster size together with the measured data (Ref. 7).

tified in the calculations. For example, for Sc_8 , the triplet and singlet two-capped octahedrons are only 0.016 and 0.024 eV higher above the quartet ground state. Similarly, the quartet state of Sc_{11} is only 0.010 eV higher than that of the doublet ground state. These energetically close isomers cannot be distinguished in Stern-Gerlach deflection experiments because of the limited resolving ability of the experimental apparatus. Therefore, “effective” magnetic moments which are spin-weighted averages over the quasidegenerate structures should be a more reasonable benchmark to which to compare to the experiment. To date, there is still a lack of a well-founded theory or model to define an “effective” magnetic moment. In this paper, the “effective” magnetic moment \bar{S} is obtained as a multiplicity-weighted average over the various quasidegenerate structures, defined as

$$\bar{S} = \frac{\sum_i (2S_i + 1)S_i}{\sum_i (2S_i + 1)}, \quad (3)$$

where S_i is the total magnetic moment of the i th low-lying isomer in spin. In Table II we present the total cluster magnetic moments, the average magnetic moment per atom of the low-lying isomers and the “effective” magnetic moments obtained via Eq. (3) together with the measured values⁷ for Sc_n clusters with $n=5-18$. The average magnetic moment per atom of the corresponding lowest energy structures, the “effective” and measured magnetic moments are also plotted as a function of cluster size in Fig. 4. It can be seen from Table II that the measured magnetic moments lie between the moments of the lowest energy structures and the alternative low-lying isomers. Clearly, the effective magnetic moments are in better agreement with the measured ones⁷ for the sizes with $n=6, 8, 14-18$ although the large discrepancy at $n=13$ remains unexplained. This failure might be due to the fact

TABLE II. The total magnetic moment (μ), the relative energy (ΔE) to the corresponding most stable structure, the average magnetic moment per atom (μ/atom), the effective average magnetic moment per atom ($\bar{\mu}/\text{atom}$), and the measured magnetic moment per atom (EXP) of the Sc_n clusters with $n=5-20$.

System	$\mu(\mu_B)$	ΔE (eV)	$\mu/\text{atom} (\mu_B)$	$\bar{\mu}/\text{atom} (\mu_B)$	Exp. (Ref. 7) (μ_B)
Sc_5	1	0	0.200	0.200	0.170 ± 0.017
Sc_6	2	0	0.333	0.250	0.218 ± 0.011
	0	0.096	0		
Sc_7	1	0	0.143	0.143	0.131 ± 0.008
Sc_8	4	0	0.500	0.361	0.246 ± 0.009
	2	0.016	0.250		
	0	0.024	0		
Sc_9	1	0	0.111	0.185	0.112 ± 0.005
	3	0.027	0.333		
Sc_{10}	2	0	0.200	0.150	0.154 ± 0.140
	0	0.010	0		
Sc_{11}	1	0	0.091	0.212	0.140 ± 0.010
	3	0.044	0.273		
Sc_{12}	4	0	0.333	0.271	0.187 ± 0.007
	2	0.052	0.167		
	0	0.085	0		
Sc_{13}	19	0	1.462	1.462	0.461 ± 0.017
Sc_{14}	8	0	0.571	0.429	0.126 ± 0.007
	2	0.032	0.142		
	0	0.070	0		
Sc_{15}	3	0	0.200	0.156	0.101 ± 0.005
	1	0.090	0.067		
Sc_{16}	0	0	0	0.094	0.076 ± 0.004
	2	0.048	0.125		
Sc_{17}	1	0	0.059	0.137	0.080 ± 0.004
	3	0.093	0.176		
Sc_{18}	0	0	0	0.160	0.167 ± 0.011
	2	0.050	0.111		
	4	0.152	0.222		

that DFT computes structures in their static states (0 K) whereas the experimental data is measured at finite temperature (58 ± 2 K).⁷ This suggests that further computations and measurements are needed to verify and understand the magnetism of Sc_{13} .

E. Transition in magnetic ordering

In order to gain more insight on the magnetic nature of Sc clusters, we have performed natural orbital population analysis (NPA) on the ground state structures. Because NPA computation is not available in DMOL package, we used the PBE

functional and the LANL2DZ basis set³¹ implemented in the GAUSSIAN-03 package instead.³² Figure 5 depicts the local atomic spins on each Sc atom for representative Sc_n clusters with $n=2, 8, 9, 13$.

Both the ferromagnetic ordering and ferrimagnetic ordering are found in the scandium clusters studied here. Notably, the spins on each Sc atom are all parallel (ferromagnetically aligned) for the clusters with $n \leq 8$. The local magnetic moment on each Sc atom is $2\mu_B$ for Sc_2 , $0.33\mu_B$ for Sc_3 , and $0.5\mu_B$ for Sc_4 and Sc_8 , respectively. The first appearance of a ferrimagnetic coupling takes place at $n=9$ which spins on two of the Sc atoms align antiparallel to those the remaining

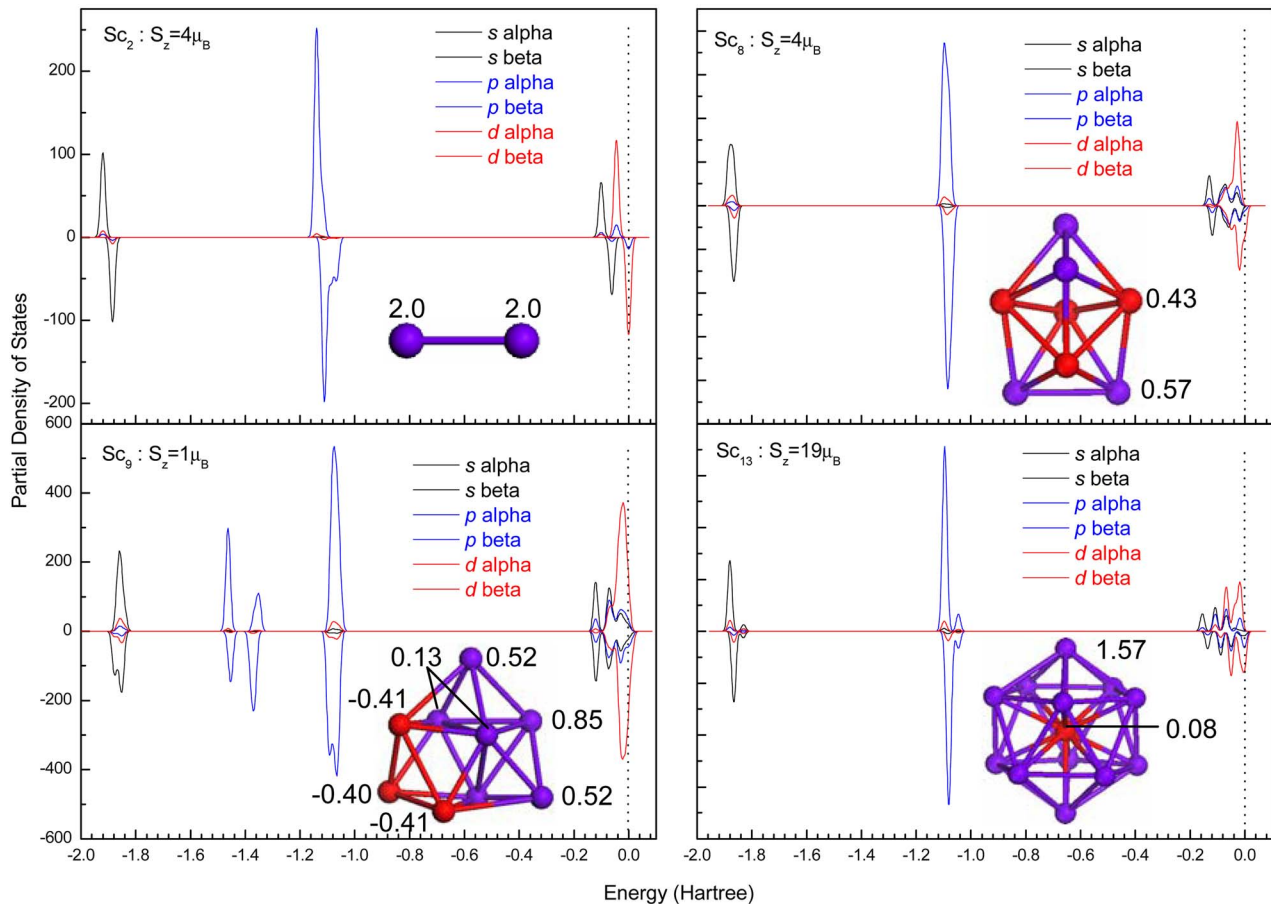


FIG. 5. (Color online) The s -, p -, d -projected partial density of states and local magnetic moment on each Sc atom computed for the lowest energy structure of representative Sc clusters with $n=2, 8, 9$, and 13 . The numerical numbers close to the structures are the atomic spin in units of μ_B . Different colors of atoms are used to distinguish the spin-up or spin-down or distinct magnetic alignments, while the dashed line refers to Fermi level which is shifted to zero.

seven atoms, with local atomic moments of the two antiparallel Sc atoms having values of $0.4\mu_B$. However, ferromagnetic ordering again prevails over the ferrimagnetic/antiferromagnetic ordering for Sc_{10} . Similar competition of these two types of magnetic ordering are observed in the range of $n=11-14$ which Sc_{11} and Sc_{12} assume ferrimagnetic coupling while Sc_{13} and Sc_{14} are ferromagnetically coupled. Particularly interesting is the case of Sc_{13} for which the atomic spin is found to be $1.57\mu_B$ for the surface atoms and close to be zero for the core atom. For $n=15-17$, ferrimagnetic ordering of Sc atoms is again energetically preferred for the ground states. The Sc_{18} cluster is found to be nonmagnetic which might indicate the approach to the nonmagnetic nature of bulk Sc. It is also noteworthy that two clusters of Sc_2 and Sc_{13} possess spins exceeding $1\mu_B$ contrary to the predictions of Hund's rule value for the isolated Sc atom.

F. Spin density and d -electron localization

Figure 5 presents the s -, p -, d -projected partial density of states (PDOS) of the majority (spin-up) and the minority (spin-down) for the lowest energy structures of Sc_n clusters

for $n=2, 8, 9, 13$. As is evident from the figure, the d -projected PDOS play a dominant role in the determination of the magnetism of the cluster whereas the s - and p -projected PDOS contribute only a small amount of net spin. This finding is also confirmed from NPA analysis. The contribution to the total magnetic moment is around 90% from $3d$ electrons whereas the contribution from $4s$ electron is less than 10%. Take Sc_{13} as an example, we find that the magnetism of Sc_{13} stems mostly from $3d$ electrons of surface Sc atom (87%) while the contribution from $4s$ electron is only about 9%. In the case of Sc_8 , in particular the contribution of $3d$ electrons to the magnetism of the cluster is nearly 98% such that the influence of $4s$ electrons can nearly be ignored.

Moreover, we find that the core Sc atoms or other atoms having high coordination numbers possess small atomic spin although they generally tend to lose more electronic charge. Returning to Sc_{13} as an example, we find that the local magnetic moment of $0.08\mu_B$ is located on the core Sc atom while $1.57\mu_B$ is obtained for the surface atoms. Similar observations can also be found at other sizes such as Sc_{14-17} which compact structures are preferred as the ground state packing and the core atom possesses nearly zero magnetic moment.

IV. CONCLUSION

In summary, we have studied the structural, energetic, electronic, and magnetic properties of Sc_n , $n=2-18$ using gradient-corrected DFT. The binding energies, the second differences of energies, and the HOMO-LUMO gaps have been investigated as function of the cluster size. The high stability of the clusters at $n=4,7,10,13,16$ can be partly attributed to the high-symmetry geometries of these clusters as well as electronic stability as predicted by the elliptical spherical jellium model. Special stability may be a result of the coexistence of atomic motif and electronic ordering with the former dominant in determining the stability of the clusters. The average magnetic moment per atom of the lowest energy structures displays size-dependent behavior and reaches the peak at $n=13$ with $\mu=1.5\mu_B$ per atom. The “effective” magnetic moments computed as the spin-weighted average over different low-lying spin states are in good accord with the measured values for most sizes. Ferromagnetic coupling is energetically preferred for clusters possessing less than nine atoms whereas ferrimagnetic / antiferromagnetic

coupling is favored for large sizes of $n=15-17$. The two types of coupling are competed in the medium-size range from $n=9-14$. The first appearance of the nonmagnetic ordering takes place at $n=18$ which might provide an evidence that the small clusters are magnetic while the bulk scandium is paramagnetic.

Note added. Recently, an additional paper on Sc_n has been published.³³

ACKNOWLEDGMENTS

This work was supported by the National Nature Science Foundation of China (Grant No. 10604013), the Program for New Century Excellent Talents in the University of China, Qinglan Project in the University of Jiangsu Province and the Teaching and Research Foundation for the Outstanding Young Faculty of Southeast University (Grant No. 4007021143). The author would thank M. B. Knickelbein and P. A. Acioli for valuable discussions. The author would also like to thank the computational resource (SGI Origin-2000 supercomputer) at Nanjing University.

-
- ¹J. A. Alonso, Chem. Rev. (Washington, D.C.) **100**, 637 (2000).
²L. A. Bloomfield, J. Deng, H. Zhang, and J. W. Emmert, in *Proceedings of the International Symposium on Cluster and Nanostructure Interfaces*, edited by P. Jena, S. N. Khanna, and B. K. Rao (World Scientific Publishers, Singapore, 2000), p. 131.
³X. S. Xu, S. Y. Yin, R. Moro, and W. A. de Heer, Phys. Rev. Lett. **95**, 237209 (2005).
⁴M. B. Knickelbein, Chem. Phys. Lett. **353**, 221 (2002).
⁵M. B. Knickelbein, Phys. Rev. B **70**, 014424 (2004).
⁶A. J. Cox, J. G. Louderback, and L. A. Bloomfield, Phys. Rev. Lett. **71**, 923 (1993).
⁷M. B. Knickelbein, Phys. Rev. B **71**, 184442 (2004).
⁸P. Bobadova-Parvanova, K. A. Jackson, S. Srinivas, and M. Horoi, J. Chem. Phys. **122**, 014310 (2005); P. Bobadova-Parvanova, K. A. Jackson, S. Srinivas, M. Horoi, C. Kohler, and G. Seifert, *ibid.* **116**, 3576 (2002); M. Kabir, A. Mookerjee, and D. G. Kanhere, Phys. Rev. B **73**, 224439 (2006); S. Polesya, O. Siper, S. Bornemann, S. J. Minar, and H. Ebert, Europhys. Lett. **74**, 1074 (2006).
⁹S. P. Walch and C. W. Bauschlicher, J. Chem. Phys. **83**, 5735 (1985).
¹⁰S. P. Walch, Theor. Chim. Acta **71**, 449 (1987).
¹¹M. Hada, H. Yokono, and H. Nakatsuji, Chem. Phys. Lett. **141**, 339 (1987).
¹²H. Akeby and L. G. M. Pettersson, J. Mol. Spectrosc. **159**, 17 (1993).
¹³H. Akeby, L. G. M. Pettersson, and P. E. M. Siegbahn, J. Chem. Phys. **97**, 1850 (1992).
¹⁴I. Papai and M. Castro, Chem. Phys. Lett. **267**, 551 (1997).
¹⁵A. Berces, Spectrochim. Acta, Part A **53**, 1257 (1997).
¹⁶Z. J. Wu, H. J. Zhang, J. Meng, Z. W. Dai, B. Han, and P. C. Jin, J. Chem. Phys. **121**, 4699 (2004).
¹⁷C. J. Barden, J. C. Rienstra-Kiracofe, and H. F. Schaefer III, J. Chem. Phys. **113**, 690 (2000).
¹⁸G. L. Gutsev and C. W. Bauschlicher, Jr., J. Phys. Chem. A **103**, 4755 (2003).
¹⁹B. N. Papas and H. F. Schaefer III, J. Chem. Phys. **123**, 074321 (2005).
²⁰J. P. Perdew, K. Burke, and M. Ernzerhof, Phys. Rev. Lett. **77**, 3865 (1996).
²¹B. Delley, Phys. Rev. B **66**, 155125 (2002).
²²DMOL is a density functional theory program distributed by Accelrys, Inc. B. Delley, J. Chem. Phys. **92**, 508 (1990); **113**, 7756 (2000).
²³NIST Standard Reference Database 69, March 2003 Release: NIST *Chemistry WebBook*; <http://webbook.nist.gov>
²⁴M. Moskovits, D. P. DiLella, and W. J. Limm, J. Chem. Phys. **80**, 626 (1984).
²⁵K. A. Gingerich, Faraday Symp. Chem. Soc. **14**, 109 (1980).
²⁶F. Cleri and V. Rosato, Phys. Rev. B **48**, 22 (1993).
²⁷D. M. Deaven and K. M. Ho, Phys. Rev. Lett. **75**, 288 (1995); J. Zhao and R. H. Xie, J. Comput. Theor. Nanosci. **1**, 117 (2004).
²⁸J. J. Zhao, Q. Qi, B. L. Wang, J. L. Wang, and G. H. Wang, Solid State Commun. **118**, 157 (2001).
²⁹R. P. Gupta, Phys. Rev. B **23**, 6265 (1989); F. Cleri and V. Rosato, *ibid.* **48**, 22 (1993).
³⁰C. Kittel, *Introduction to Solid State Physics*, 7th ed. (Wiley, New York, 1996).
³¹P. J. Hay and W. R. Wadt, J. Chem. Phys. **82**, 270 (1985); **82**, 284 (1985); **82**, 299 (1985).
³²M. J. Frisch *et al.*, GAUSSIAN 03, Gaussian, Inc., Pittsburgh, PA, 2003.
³³H. K. Yuan, H. Chen, A. S. Ahmed, and J. F. Zhang, Phys. Rev. B **74**, 144434 (2006).